

IPC2006-10172

CRACK TIP OPENING ANGLE: MEASUREMENT AND MODELING OF FRACTURE RESISTANCE IN LOW AND HIGH STRENGTH PIPELINE STEELS*

Ph. P. Darcis

NIST, Materials Reliability Division (853), 325
Broadway, Boulder, CO 80305-3328 USA
NIST, Metallurgy Division (855), 100 Bureau Drive,
Gaithersburg, MD 20899-8555 USA
darcis@boulder.nist.gov

G. Kohn and A. Bussiba

NIST, Materials Reliability Division (853), 325
Broadway, Boulder, CO 80305-3328 USA
NRCN , P.O. Box 9001 , Beer-Sheva, Israel

J. D. McColskey, C. N. McCowan
and T. A. Siewert
NIST, Materials Reliability
Division (853), 325 Broadway,
Boulder, CO 80305-3328 USA

R. Fields

NIST, Metallurgy Division (855),
100 Bureau Drive, Gaithersburg,
MD 20899-8555 USA

R. Smith and J. Merritt

DoT, Office of Pipeline Safety
400 7th Street, S.W.
Washington D.C. 20590 USA

ABSTRACT

Crack tip opening angle (CTOA) is becoming one of the more widely accepted properties for characterizing fully plastic fracture. In fact, it has been recognized as a measure of the resistance of a material to fracture, in cases where there is a large degree of stable-tearing crack extension during the fracture process. This type of steady-state fracture resistance takes place when the CTOA in a material reaches a critical value, as typically occurs in low-constraint configurations. Our current research has applied the CTOA concept as an alternative or an addition to the Charpy V-notch and the drop weight tear test (DWTT) fracture energy in pipeline characterization. A test technique for direct measurement of CTOA was developed, using a modified double cantilever beam (MDCB) specimen. A digital camera and image analysis software are used to record the progression of the crack tip and to estimate CTOA using the crack edges adjacent to the crack tip. A steady-state CTOA has been successfully measured on five different strength grades of gas pipeline steel (four low strength grades and one high strength grade: X100). In addition, two-dimensional finite element models (2D FEMs) are used to demonstrate the sequence of the fracture process and the deformation mechanisms involved. The CTOA measurements and models are correlated and agree well.

INTRODUCTION

The increasing demand for natural gas as an alternative energy source implies continued growth of gas pipeline installations and the need for construction of new, large-diameter pipelines. This trend compels the natural gas transmission industry to consider higher operating pressures (more than 15 MPa). The application of high strength steels in severe conditions will require reliable pipeline designs, as well as inspection and maintenance procedures that will prevent in-service failures. A difficult problem to be solved for the economic and safe operation of high pressure gas pipelines is the control of ductile fracture propagation. In this case, a safety factor must be calculated in terms of fracture arrest capability. As a result, the accurate prediction of the resistance to fracture, namely the ductile fracture arrest of the pressurized pipeline, is now one of the urgent issues to be solved for the transmission of natural gas. Ductile fracture must be considered in gas pipelines to predict the extent of damage a pipeline would suffer if a crack is started by an unexpected stress source (i.e. third party damage).

The concept of overall absorbed fracture energy was traditionally used to design low strength grade pipeline steels against ductile fracture. Initially, the measure of material fracture resistance was constructed on the basis of Charpy V-notch (CVN) shelf energy, like the Battelle two curve model (TCM) [1]. Later fracture arrest/propagation models were calibrated against dynamic drop weight tear test (DWTT) data

* Contribution of an agency of the U.S. government, not subject to copyright

as the full wall thickness fracture surface of this specimen better represented the shear characteristics of the pipe. These failure models worked well for low toughness steels (below 550 MPa yield, Charpy toughness level up to 95 J) [2], but needed corrections for high toughness steels.

It has become clear that extrapolating the existing experimental absorbed fracture energy relations, to assess the fracture resistance of higher strength grades of modern pipeline steels, introduces significant errors [2-4]. Some correction factors were suggested [3,4] to set toughness requirements for high strength grade steels. However, the addition of correction factors may not capture the fracture mechanisms for the fracture phenomenon observed.

In parallel to the CVN and DWTT based fracture strategies, pipeline designers have worked on developing new measures of fracture control. Among these, crack tip opening angle (CTOA) which is based on the crack opening displacement (COD) ductile fracture criterion, is becoming one of the more widely accepted properties for characterizing fully plastic fracture [5-8]. The main advantages of CTOA are that it can be directly measured from the crack opening profile and can also be related to the geometry of the fracturing pipe. Furthermore, in cases where there is a large degree of stable-tearing crack extension during the fracture process, CTOA has been recognized as a measure of the resistance of a material to fracture. This type of steady-state fracture resistance takes place when the CTOA in a material reaches a critical value, as typically occurs in low-constraint configurations. This suggested that a steady-state CTOA could be considered to be a material property and used as either an addition or an alternative to the absorbed fracture energy for the assessment of the toughness of pipeline steels. In addition, the CTOA criterion can be implemented easily in finite element models of the propagating fracture process.

Our current research has applied the CTOA concept (using a single specimen CTOA test method and CTOA FEM modeling) to determine the properties of low and high strength grade pipeline steels (X100 steel). A test approach for direct measurement of the material CTOA was developed based on a modified double cantilever beam (MDCB) specimen. This test technique utilized optical imaging (digital and video cameras) to record images of the crack tip for post-analysis of the CTOA of each material studied. The angle of the deformed gridlines near the crack tip as well as the angle of the crack edges were measured during crack extension from the captured images. A plot of CTOA versus crack length was generated to obtain the critical CTOA ($CTOA_c$), which represents the material fracture toughness. In addition, 2D FEM CTOA models are used to demonstrate the sequence of the fracture process and the deformation mechanisms involved. The CTOA measurements and models are correlated.

MATERIAL PROPERTIES

Five pipeline steels were investigated: four used and unused (as manufactured) low strength grade pipeline steels, # 1 to 4, and one high strength grade pipeline steel (# 5; 52 inch (1.32 m) O.D. x 20.6 mm). Table 1 contains the chemical composition of the steels (weight %).

Table 1. Chemical composition of the tested steels (weight %)

Steel #	C	Co	Cr	Cu	Mn	Mo
1	0.06	0.006	0.020	0.110	1.46	0.025
2	0.24	0.025	0.024	0.038	1.03	0.016
3	0.27	0.007	0.029	0.015	0.36	0.007
4	0.18	0.014	0.021	0.540	0.52	0.009
5	0.07	N/A	N/A	0.300	1.90	0.150

Steel #	Nb	Ni	P	S	Si	V
1	0.054	0.100	0.010	<0.010	0.280	0.045
2	0.007	0.064	0.016	0.0130	0.057	0.002
3	0.005	0.021	0.005	0.0150	0.009	0.003
4	0.005	0.021	0.026	0.0100	0.043	-
5	N/A	0.500	0.008	0.0005	0.100	N/A

As shown in Table 1, steels # 1 and 5 are characterized by low C, whereas the other steels (# 2 - 4) contain higher C and S, typical of older pipeline steels. Only three of the five steels are identified with a grade designation, and only three of them were used in service. Table 2 summarizes their properties.

Table 2. Designation and remarks of the tested steels

Steel #	1	2	3	4	5
Designation	N/A	X52	Grade B	N/A	X100
O. D. (inch)	20	20	22	20	52
O. D. (m)	0.51	0.51	0.52	0.51	1.32
Thickness (mm)	11.4	8.1	8.1	8.1	20.6
Remarks	Unused	Used	Used	Used	Unused*

* pressure tested

To measure the pipelines tensile properties, flat tensile specimens were machined from pipeline steels # 1-4, and round tensile specimens (6 mm diameter) were machined from the X100 steel (steel # 5). The flat specimens were 6 mm wide and the full thickness for the longitudinal orientation, and typically 3 mm thick for the transverse specimens. Specimens were machined in both axial (longitudinal) and transverse orientations, and all specimens had a gauge length of 25.4 mm. Experiments were performed in a screw driven tensile testing machine of 100 kN capacity, and a closed-loop servo-hydraulic machine of 100 kN capacity. Tests were conducted in displacement control at rates of 0.25 mm/min (for steels # 1-4) and 0.1 mm/min (for steel # 5). The differences in specimen

shapes and displacement are not expected to have much effect on the mechanical properties.

The measured mechanical properties of the five steels are shown in Table 3, where E is the Young modulus, $\sigma_{0.2}$ the yield stress, σ_{UTS} the ultimate strength, e_u the uniform elongation, and e_f the fracture elongation. In addition to the Young modulus given by the stress-strain curves (which can be subject to specimen effects like outside corrosion), dynamic elastic modulus measurements for the samples taken from the different pipeline steels # 1 - 4 were conducted according to standard ASTM E1876-01 [9]. Table 4 summarizes three dynamic elastic modulus measurements: $E(1)$, measured for out of plane flexure which has the greatest strains on the wide flat sides, $E(2)$, measured for in-plane flexure which has the greatest strains on the long edges, and $E(3)$, measured for longitudinal vibrations with equal strains across the cross section.

Table 3. Mechanical properties in transverse and longitudinal direction

Steel #	Orientation	E (GPa)	$\sigma_{0.2}$ (MPa)	σ_{UTS} (MPa)	$\sigma_{0.2}/\sigma_{UTS}$
1	L	201	517	611	0.85
	T	231	543	606	0.90
2	L	186	360	556	0.65
	T	214	448	576	0.78
3	L	184	244	451	0.54
	T	189	255	459	0.56
4	L	174	335	535	0.63
	T	199	428	560	0.76
5	L	199	694	801	0.87
	T	235	797	828	0.96

Steel #	Orientation	e_u (%)	e_f (%)	e_u/e_f
1	L	6.7%	35.0%	0.19
	T	8.0%	27.4%	0.29
2	L	12.3%	32.7%	0.38
	T	11.1%	25.6%	0.43
3	L	19.6%	37.8%	0.52
	T	18.8%	38.0%	0.49
4	L	12.9%	34.9%	0.37
	T	10.5%	22.0%	0.48
5	L	4.3%	25.0%	0.17
	T	4.3%	24.5%	0.17

Table 4. Three dynamic elastic modulus measurements

Steel #	1	2	3	4	5
$E(1)$ (GPa)	212.2	210.9	213.3	210.5	N/A
$E(2)$ (GPa)	210.0	212.8	211.5	211.5	N/A
$E(3)$ (GPa)	211.1	209.6	211.5	209.7	N/A

In addition to the standard properties, the ratios of $\sigma_{0.2}/\sigma_{UTS}$ and e_u/e_f are also given in Table 3. These two parameters indicate the strain hardening potential of the steel. As shown in Fig. 1, as the stress ratio increases the strain ratio decreases, with a moderate trend for the longitudinal direction and a slightly steeper trend for the transversal direction. The ratio values for the various pipes are also given for both longitudinal and transversal curves.

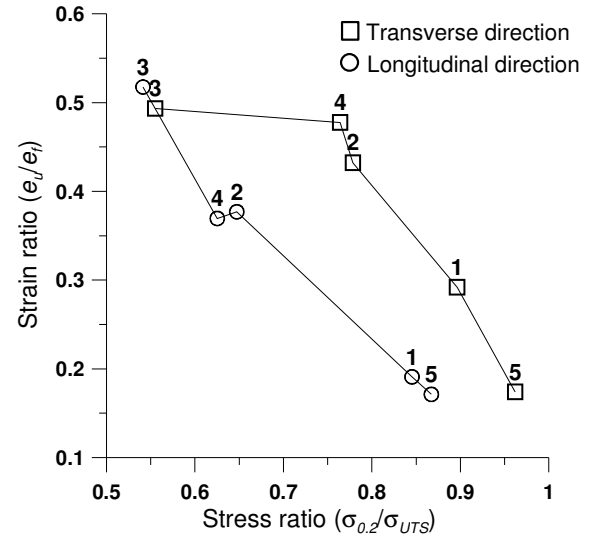


Figure 1. Dependency of the strain ratio with the stress ratio for both orientations (steel numbers from Tables 1 to 4)

CTOA SPECIMEN AND TEST SET UP

A modified double cantilever beam (MDCB) specimen was used to conduct the CTOA Test. This specimen was proposed by several authors [2,10,11]. The MDCB specimen is designed primarily to prevent bending as well as tension loads, which have been experienced in both standard and tapered DCB. So the modified specimen exhibits the following characteristics:

- It may be cut directly from a pipe, without any flattening.
- The maximum possible width, thickness and ligament provide a large plastic zone. The width and thickness are limited by pipe curvature and wall thickness.
- High constraint in the test section is promoted by two thicker loading arms. This serves two purposes. First, positive or at least non-negative longitudinal strains can be achieved, and second, the loading is predominantly in tension with only a small shear component.
- The test section does not restrain the transition to slant mode shear fracture.
- The test section is flat near the crack tip for ease of CTOA measurement.

Two MDCB configurations and dimensions are depicted in Fig. 2. The first, shown in Fig. 2a, was used for the thin walled pipes ($\times 8.1$ and 11.4 mm, steels # 1-4) and the second, Fig. 2b,

was used for the thicker-wall X100 ($\times 20.6$ mm, steel # 5) pipe. Initially, the crack mouth opening displacement (CMOD) gauge was attached at the mouth of the notch and was later attached adjacent to the fatigue crack, hence the difference in the notch openings between those shown in Figs. 2a and 2b.

The large in-plane dimensions of the specimens (200 mm \times 100 mm) and the long ligament allowed relatively large amounts of stable crack growth. To increase the restraint effects in the high strength grade steel specimens, the arm thickness of the specimens was increased (see details in Fig. 2b). This resulted in two thick loading arms and a thin flat side-grooved region on opposite sides of each specimen. The flat side-grooved region was used to study crack growth and for optical measurement of CTOA values.

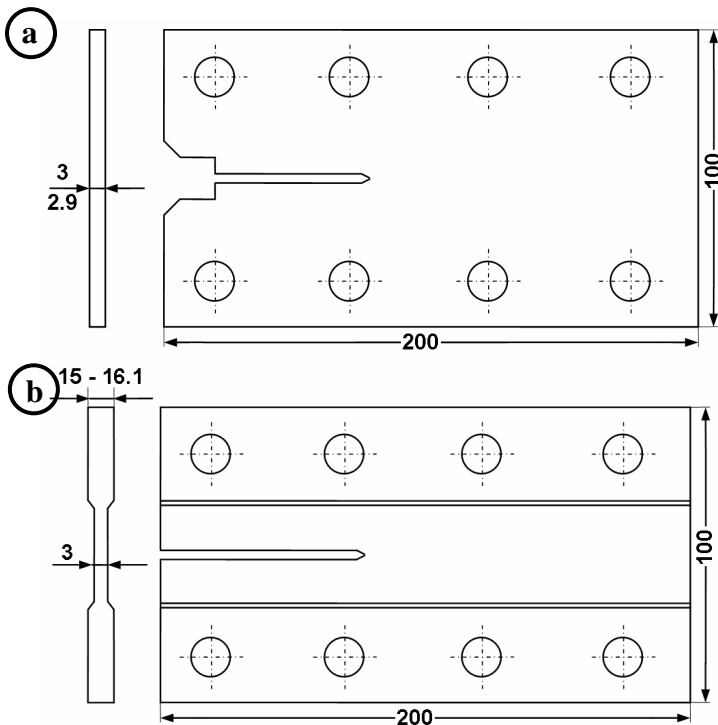


Figure 2. MDCB specimens, configurations and dimensions (in mm)

Test specimens were extracted from plate cut from the longitudinal axis of the pipe. The thickness of the curved plate was reduced by machining to obtain a flat plate. This eliminated the probable residual plastic strains that would be caused by flattening the plate by use of a straightening procedure. Eleven specimens were extracted from pipelines in the T-L orientation, where T is the transverse and L the longitudinal orientation. A schematic of the specimen-cutting scheme is shown in Fig. 3.

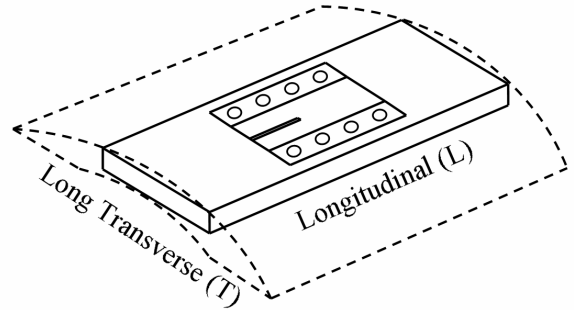


Figure 3. Orientation of CTOA specimen in the pipe

An initial straight notch (1.6 mm width) was machined through the specimen thickness. The notch length was 60 mm (measured from the load-line of the pins).

The loading of the specimen was conducted using a pair of thick plate grips bolted to the side surfaces of the specimen (Fig. 4). Two cylindrical pins provided free rotation of the whole assembly (specimen plus loading plates) during the experiments (Fig. 4). The thin flat side-grooves together with the two thick loading plates increased the constraint levels in the gauge section. The long uncracked ligament and the loading geometry provided the condition of stable shear crack extension in the specimen ligament similar to that of the real structure. The load-line passes between the left pair of loading holes.

A fine square mesh, with a spacing of 1.27×1.27 mm (0.05×0.05 in), was scribed on the side surfaces of each specimen to facilitate the CTOA measurement. The square grid was scored on the specimens with a milling machine having ± 0.01 mm accuracy.

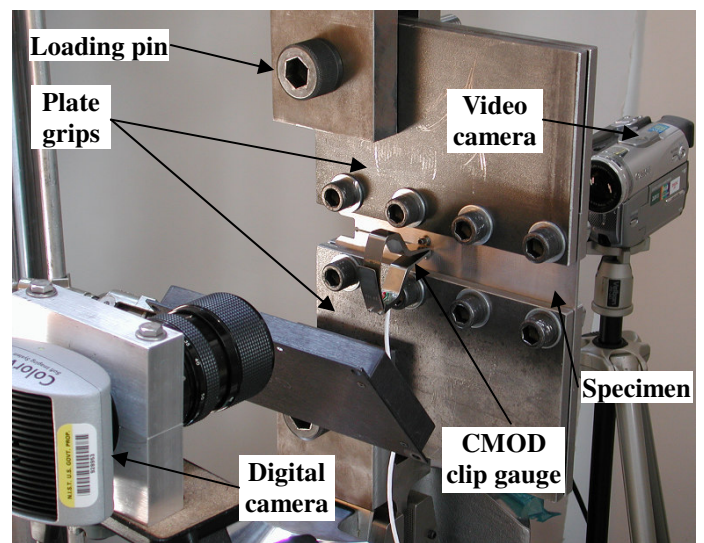


Figure 4. CTOA test set up

MECHANICAL TEST CONDITIONS

The experiments were conducted on a 250 kN closed loop servo-hydraulic test machine, under opening (mode I) loading and quasi-static conditions, at a low strain rate under displacement control in the range of 0.02 to 0.05 mm/s. In each test, the time, load, load line displacement, and CMOD gauge were recorded (see Fig. 4 for the test set up).

The specimens were first fatigue pre-cracked following the ASTM standard procedure for conducting crack tip opening displacement (CTOD) tests [12]. The pre-cracking loads were selected by keeping the ratio of stress intensity factor range to the Young modulus ($\Delta K/E$) below $0.005 \sqrt{\text{mm}}$. All specimens were fatigue pre-cracked at a ratio of $R = 0.1$ [13], to a crack-to-width ratio of $a_0/W = 0.3$ to 0.5 (with a specimen width, W , equal to 182 mm, and a_0 equal to the machined notch length (60 mm) plus the initial fatigue pre-crack length).

After the fatigue pre-cracking, the specimens were slowly pulled apart, causing the growing crack to tear before reaching maximum load and transitioning to a state of stable tearing.

Two tests were conducted on steel # 1, three on steel # 2; two on steel # 3; one on steel # 4 and two on steel # 5. Table 5 summarizes the specimen specifications.

Table 5. Specification of the CTOA specimens (for the 5 different steels referenced in Tables 1, 2, 3 and 4)

Steel #	Specimen gauge thickness (mm)	Pipeline thickness (mm)	Ratio specimen gauge to pipeline wall thickness	Displacement rate (mm/s)
1	2.9	11.4	25 %	0.05
2	2.9	8.1	36 %	0.05
3	2.9	8.1	36 %	0.05
4	2.9	8.1	36 %	0.05
5	3.0	20.6	15 %	0.02

Steel #	Arm thickness (mm)	Ratio specimen gauge to arm thickness	Initial fatigue pre-crack length (mm)	a_0/W ($W = 182 \text{ mm}$)
1	2.9	100 %	16.5	0.42
2	2.9	100 %	7.2	0.37
3	2.9	100 %	11	0.39
4	2.9	100 %	3	0.35
5	15.6	19 %	7.8	0.37

CTOA MEASUREMENT

Several methods exist to measure the CTOA. Some are direct methods using moiré interferometry [14], optical microscopy [2,15,16], or digital image correlation, and others are indirect methods using microtopography [16] or experimental force-displacement diagrams [16]. Both direct and indirect methods are included in the ISO and ASTM draft

standards for CTOA testing (two direct and two indirect methods corresponding to reference 15).

For our study an optical method was used. A digital camera, mounted on an xyz-stage (Fig. 4) was controlled by a personal computer and image analysis software. The captured images had a size of 2048×1536 pixels with a resolution of about 32 micrometers per pixel. Images were acquired and stored along with time, load, displacement and clip gauge (CMOD) data by the software as the crack propagated across the double cantilever beam CTOA specimen.

A digital video camera (Fig. 4) with a resolution of 320×240 pixels was used on the back side of the specimen to record the test as a back-up. This video also provides a continuous record for the test.

The CTOA was measured with software developed for this study. The program requires the operator to indicate (mouse position) the crack tip position and positions along the crack faces near the tip, or grid locations. For this semi-automatic approach, the goal was to limit the input required by the operator and optimize the algorithm(s) used to calculate the CTOA for the test. The captured images were analyzed approximately every 0.5 mm of crack growth. In each image, both direct (crack face positions) and indirect (grid positions) methods were used to determine the CTOA, but only the results of direct measurements are reported here. The direct measurement for CTOA at the crack tip edges were made in accordance with the optical method referenced in the ISO and ASTM draft standards [16]. An example of crack tip location and CTOA measurement are shown in Fig. 5.

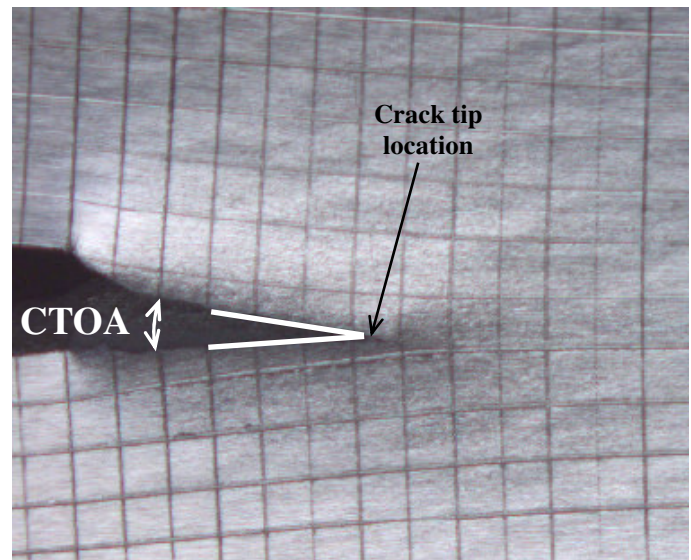


Figure 5. Crack tip location and CTOA measurement

CTOA TEST RESULTS AND DISCUSSION

Extensive combinations of experimental and computational work on gas pipeline steels by Mannucci et al. [7], Wilkowski et

al. [8] and others show that the CTOA data approach a plateau during the steady state phase of shear crack propagation. This steady CTOA, considered as a material property, is generally preceded by relatively high CTOA values during the early stages of cracking after the crack has grown several times the specimen thickness. These two behaviors are also observed in all our tests.

Figure 6 illustrates the CTOA resistance curves for high strength pipeline steel (X100 steel). This figure represents the CTOA results from more than 125 images captured from two CTOA specimens.

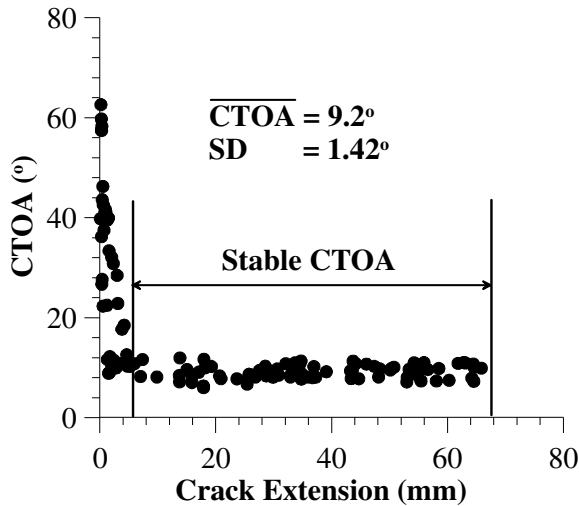


Figure 6. CTOA resistance curves for X100 steel

In Fig. 6, the initiation CTOA was high (around 60°) and it rapidly dropped in the flat-to-slant fracture transition region and approached a constant value (associated with steady state crack growth) at a crack length of 1.5 times the specimen thickness. Flat tearing and tunneling effects dominated the non-constant CTOA profile during the early stages of crack growth. After the transition, full slant tearing (shear mode) was developed and resulted in a steady state CTOA value. The average maximum load reached in the two tests (steel # 5 corresponding to X100) was 59.6 kN, and the maximum crack velocity during the test reached 0.65 mm/s.

The CTOA resistance value of 9.2° for the X100 steel is consistent with the CTOA data of 8.6° reported by Hashemi et al. [2] (measured with a similar quasi-static test technique, with specimen thickness of 8, 10 and 12 mm, and a similar measurement technique: an optical microscopy method with a digital video camera), for a different X100 steel. Furthermore, the comparison of the X100 results from the technique described here with those from drop-weight tear tests (Mannucci et al. [17]), that involve rapid loading values, and from tests on full pipes (Berardo et al. [18]) shows that the data are very comparable for each material class. Mannucci reported a CTOA value of 7° (measured by two specimen tests) and 9.8° (estimated by FEA), for a different X100 steel. Berardo

reported CTOA results between 8.6° and 9.6°, measured from the displacement field behind the crack tip (reconstructed from the strain gauge records obtained during the full scale burst test for a different X100 steel). These data are encouraging and provide a better understanding of how the data from different test methods actually relate to each other.

A summary of the average results for the steels is given in Table 6, and strength versus CTOA is plotted Fig. 7.

Table 6. CTOA tests results (for the 5 different steels referenced in Tables 1, 2, 3 and 4)

Steel #	Stable CTOA average (°)	Stable CTOA standard deviation (°)	Maximum load (kN)	Specimen thickness times of the CTOA stabilization	Maximum crack velocity (mm/s)
1	11.7	2.04	31.0	1.9	0.22
2	9.1	1.71	31.1	1.7	0.26
3	9.8	1.39	21.0	0.54	0.22
4	10.0	2.00	30.5	0.5	0.35
5	9.2	1.42	59.6	1.5	0.65

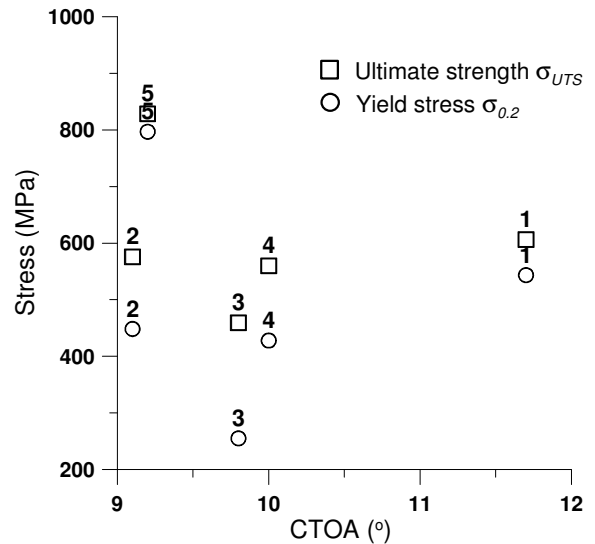


Figure 7. Stress (T direction) versus CTOA

From the results shown in Table 6 and Fig. 7, several remarks can be made:

- The X100 steel (steel # 5), which has a ferrite-bainite microstructure, has reasonably good resistance to crack growth, compared with the more traditional ferrite-pearlite pipeline steels (steel # 1-4), and this steel was characterized by higher strength.
- The lower carbon, fine grained ferrite-pearlite pipeline steel (# 1), has the highest resistance to crack growth of the steels tested here, as might be expected. This microstructure provides a good balance of toughness and strength.

- The lowest CTOA, 9.1° , is associated with the 0.24 C ferrite-pearlite steel # 2. This result is most easily compared with steel # 4, because of the similar strength levels and microstructures for the 2 steels. In this comparison, the steel with the lowest alloy content is expected to have the better resistance to crack growth (assuming the strengthening contributions for this steel rely on grain size control).

- The standard deviation (SD) in CTOA measurement is significant (between 1.3° and 2.1°). This scatter was due primarily to locating the auxiliary points on the irregular crack edges and also to uncertainty in identifying the crack tip. More accurate image acquisition systems and more robust measurement procedures are needed to reduce the scatter.

- The maximum load obtained during the test was proportional to the transverse yield stress measured during tensile testing. Steel # 3 was the lowest ($\sigma_{0.2} = 255$ MPa), with a maximum CTOA load of 21 kN, and steel # 5 was the highest ($\sigma_{0.2} = 797$ MPa), with a maximum CTOA load of 59.6 kN.

- The flat-to-slant fracture transition region occurs within 0.5 to 2 times the specimen thickness, which is sooner (1-3 times) than that for other references [2,5].

- The maximum crack velocities measured during testing were relatively constant (between 0.22 and 0.35 mm/s) for the first four steels and increased (0.65 mm/s) for steel # 5, although this test was done at a lower displacement rate (Table 5). This is due to the two thicker specimen arms, which increase the test section constraint (by increasing the thickness). Furthermore, the lower ductility in steel # 5 (X100) contributes to the higher velocity.

FINITE ELEMENT ANALYSES

An elastic-plastic finite element code, FRANC2D/L (FRacture ANalysis Code 2-D/Layered) [19,20], was used to predict the stable tearing behavior in the MDCB fracture tests. The elastic-plastic analysis employs the initial stress concept based on incremental flow theory and the assumption of small strain. A multi-linear representation of the uniaxial stress-strain curve was used in the analysis with the Von-Mises yield criterion.

The finite element models were composed of two-dimensional triangular elements (6 nodes) in the center (MDCB specimen), and two-dimensional quadrilateral elements (8 nodes) elsewhere (plate grips). The mesh pattern for the MDCB with the plate grips used for the steels # 1-4 simulations is shown in Fig. 8 (the shape of the MDCB changes for the steel # 5 simulation, see Fig. 2). A thickness of 2.9 or 3 mm (see Table 5) was used in the center mesh part, and plate grips with a thickness of 20 mm (2×10 mm) were used and added in the other mesh parts. Because the cracked, thin-sheet material exhibits predominately plane stress behavior, the central mesh part was assumed to be under plane stress conditions (area of the MDCB specimen without plate grips), and the plate grip mesh parts were assumed to be under plane strain conditions

(see Fig. 8). Fixed displacement boundary conditions were assumed at the lower plate grip hole, and monotonic load (displacement control) was applied at the upper plate grip hole. The mesh, for the simulation of steels # 1-4, had 1,222 elements and 2,865 nodes, and the mesh, for the simulation of steel # 5, had 1,248 elements and 2,919 nodes. Symmetry was not assumed about the X-axis to allow crack bifurcation and to extend our model to a non-symmetric crack configuration. Mesh patterns, in the assumed crack path extension, were selected so that the size distance between two nodes of a mesh element was 0.8 mm, in the crack tip region. This distance was selected from a previous study [21].

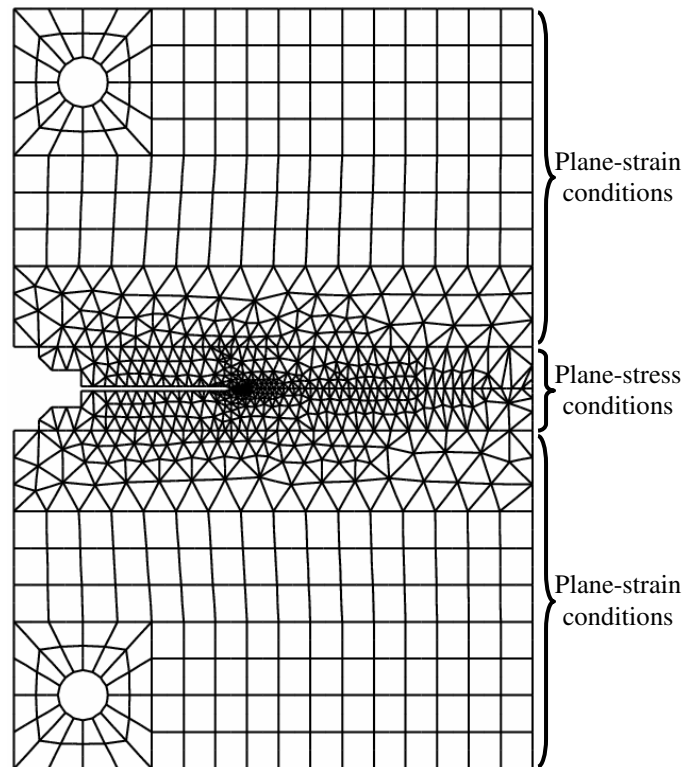


Figure 8. Finite element model for MDCB with plate grip configurations (used for simulation of steels # 1-4)

In the finite element analysis, a constant critical value of CTOA ($CTOA_c$) was chosen as the fracture criterion. The critical CTOA criterion is also equivalent to a critical crack tip opening displacement ($CTOD_c$) value at a specified distance (d) behind the crack tip since $CTOA_c = 2 \tan^{-1} [CTOD_c/(2d)]$ (the location where the angle is measured is “twice” the smallest element size along the crack line). Whenever the CTOA was greater than or equal to a preset critical value ($CTOA_c$) during incremental loading, the crack-tip node was released and the crack advanced. As allowed in the CTOA algorithm implemented in FRANC2D/L, when the angle made by points on the upper and lower crack surfaces, at a distance $d = 1.02$ mm (0.04 inch) behind the crack tip, reaches the

$CTOA_C$ critical value, the crack advanced by 2 element lengths. The advance of 2 element length crack was selected according to mesh convergence studies [20]. The 1.02 mm distance selection was based on previous analysis experience [22] (this location was chosen to match the average location where the critical $CTOA$ values were measured in the tests), and on mesh convergence studies [23]. The $CTOA_C$ values used in this study are shown in Table 6.

FEM RESULTS AND DISCUSSION

The critical $CTOA$ fracture criterion and a two-dimensional elastic-plastic finite element analysis were used to calculate the maximum applied load and the crack extension behavior (the load-line displacement was also available but not presented here). The stabilized surface $CTOA$ values (Table 6), measured by optical microscopy, were used as the critical angle.

The load – crack extension behavior for the MDCB specimens are shown in Figs. 9 and 10.

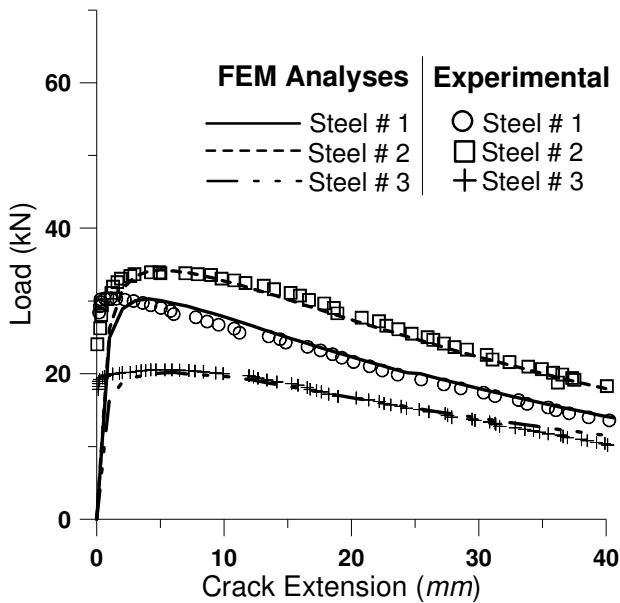


Figure 9. Load versus crack extension from experimental and FEM analyses for steels # 1-3 MDCB specimens

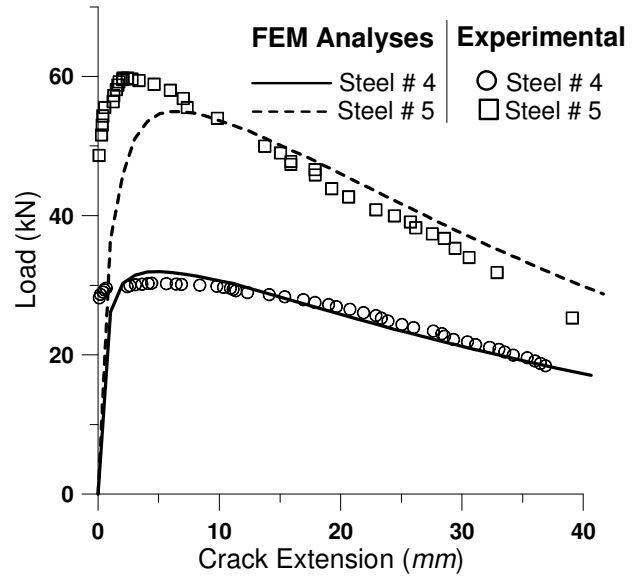


Figure 10. Load versus crack extension from experimental and FEM analyses for steels # 4-5 MDCB specimens

Table 7 summarizes the results for each steel.

Table 7. Comparison between FEM calculated and measured results.

Steel #	Maximum loading (kN)			Correlation coefficient for curves
	Experimental data	FEM data	Relative error	
1	30.4	30.3	0.29 %	0.982
2	33.9	34.3	1.04 %	0.993
3	20.6	20.2	1.82 %	0.988
4	30.3	32.0	5.56 %	0.985
5	59.8	55.0	8.03 %	0.952

From the results shown in Figs. 9 and 10 and in Table 7, several remarks can be made:

- The FEM calculated crack extension behavior (Figs. 9 and 10) for plane stress analysis (in the cracked region) agreed well with the experimental measurements. Correlation coefficients between the experimentally measured crack extension and the finite element analysis calculation for the 5 different steels tested lay between 0.952 to 0.993.

- The plane stress finite element calculation slightly underpredicted and overpredicted the experimentally measured maximum applied load at short and long crack extensions, respectively. The relative maximum load error was negligible for steels # 1-3, and increased with steel # 4 and 5. The relative error concerning the X100 steel (# 5) could be due to a misunderstanding of the steel mechanical properties (a stress-strain curve in the transverse direction may not be sufficient to take into account the specimen strain triaxiality behavior), or it could be due to stress triaxiality not taken into account in the

2D FEM simulations. This could be improved using new stress-strain characterization and 3D FEM simulations.

- The analyses tend to underpredict the initial crack extension when the crack extension is less than 6 mm (corresponding to twice the specimen thickness). This could be due to several factors:

- the experimental measurements were made from surface observations and significant crack tunneling was shown to occur in this region;
- during the phase between initiation and the attainment of maximum load, CTOA did not appear to be constant for these materials (some materials could have constant CTOA and others not during the flat-to-slant transition [21]);
- stress triaxiality could be a significant issue at the tip of the crack during the initial crack extension.

The two previous observations were not taken into account in the 2D simulation.

- The analyses accurately describe the crack extension behavior beyond the peak stress.

- Stress triaxiality is a significant issue at the tip of a crack even for thin sheet material. This stress triaxiality, or constraint, has received much attention in the past fifteen years [5,17-24]. The plane stress approximation has no constraint and the plane strain approximation introduces too much constraint (allowing the plane strain triaxiality to extend exceedingly far away from the crack tip), Newman et al. [24] modeled constraint, using the Plane Strain Core (PSC) concept, as a simple mixed state of stress with plane strain elements near the tip and plane stress elements away from the tip. The PSC concept in the 2D FEM CTOA simulations was not useful in our model. Indeed, the two thick loading arms (89.5 % of the finite element model), modeled with plane strain elements, appeared to balance the usual overestimation due to use of the plane stress elements. This is an interesting phenomenon and needs further investigation.

SUMMARY AND CONCLUSIONS

The stable tearing behavior of five different pipeline steels was investigated with a modified double cantilever beam, MDCB, specimen. A test technique for direct measurement of the steady state CTOA was presented. Optical imaging was used to record the uniform deformation of a crack edge on a specimen surface. The CTOA at the crack tip was measured during crack growth using captured images. The technique was used to determine the steady state CTOA of four low strength grades and one high strength grade (X100) gas pipeline steel. CTOA values were found to be high during the early stages of cracking, and stabilized after the crack had grown about 0.5-2 times the specimen thickness (flat-to-slant fracture transition region). In all experiments, the test method generated steady state CTOA values. The irregular crack edges and the difficult crack tip identification caused a significant CTOA standard

deviation (this could be reduced by a more accurate image acquisition system). A reasonably good resistance to crack growth for X100 steel (steel # 5) compared with the more traditional pipeline steels (steel # 1-4), was found. Maximum loads were proportional to the transverse yield stress of the various grades of steel. The maximum crack velocities were relatively constant, except for the X100 steel, which was slightly larger. The CTOA resistance value for the X100 steel (9.2°) was consistent with data reported for quasi-static tests [2], for dynamic tests (drop-weight tear tests [17]) and for full pipeline tests [18].

A bi-dimensional elastic-plastic finite element code (FRANC2D/L [19,20]), with the critical CTOA fracture criterion and plane stress (in the MDCB center) and plane strain (elsewhere) elements, was used to predict the stable tearing behavior for MDCB specimens made of 2.9 and 3 mm thick steel (for the five different steels). The analysis predicted the load and the crack extension. The constant critical CTOA, obtained from experimental measurements made on a stably tearing crack, was used. When the CTOA reached the preset critical value ($CTOA_c$), the crack-tip node releases, and the crack advances two element lengths for a length of $d = 1.02$ mm (0.04 inch), as shown in previous studies results [20-22]. The calculated crack extension behavior agreed well with the experimental measurements. The FEM model underpredicted the initial crack extension, when the crack extension was less than twice the specimen thickness, and accurately described the crack extension behavior beyond the peak stress. The plane stress finite element calculation (cracked region) slightly underpredicted and overpredicted the experimentally measured maximum applied load. These results are encouraging and stimulate us to better understand stress triaxiality at the crack tip.

The constant CTOA concept has been successfully measured and used to predict the residual strength of laboratory specimens of five pipe steels. Further CTOA measurements and finite element analyses need to be conducted at other displacement rates, thicknesses, materials and test configurations to better evaluate the constant CTOA fracture criterion.

ACKNOWLEDGMENTS

The support of British Petroleum is gratefully acknowledged for contributing the high strength pipeline steel, and for the permission to publish this work.

The support of USA Department Of Transportation, Pipeline and Hazardous Materials Safety Administration, is also gratefully acknowledged.

The efforts of Dr Richard E. Ricker, Metallurgy Division, NIST, for conducting dynamic Young modulus measurements on the pipeline steels is appreciated

REFERENCES

- [1] Rothwell, A. B., 2000, "Fracture Propagation Control for Gas Pipelines - Past, Present and Future", Pipeline Technology, 1, Denys R., eds., Elsevier Science, pp. 387-405.
- [2] Hashemi, S. H., Howard, I. C., Yates, J. R., Andrews, R. M., and Edwards, A. M., 2004, "A Single Specimen CTOA Test Method for Evaluating the Crack Tip Opening Angle in Gas Pipeline Steels", Proc. 5th International Pipeline Conference, paper No. IPC04-0610, Calgary, Alberta, Canada.
- [3] Demofonti, G., Mannucci, G., Spinelli, C. M., Barsanti, L. and Hillenbrand, H. G., 2000, "Large Diameter X100 Gas Linepipes: Fracture Propagation Evaluation by Full-Scale Burst Test", Pipeline Technology, Denys R., eds., Elsevier Science, pp. 509-520.
- [4] Leis, B. N., Eiber, R. J., Carlson, L., and Gilroy-Scott, A., 1998, "Relationship between Apparent (Total) Charpy Vee-Notch Toughness and the Corresponding Dynamic Crack Propagation Resistance", Proc. 2nd International Pipeline Conference, ASME, Calgary, Alberta, Canada, 2, pp. 723-731.
- [5] Newman, J. C. Jr., and James, M. A., 2001, "A Review of the CTOA/CTOD Fracture Criterion – Why It Works!", Proc. 42nd AIAA/ASME/ASCE/AH/ASC Structures, Structural Dynamics, and Materials Conference and Exhibit, paper No. AIAA-200-1324, Seattle, Washington, U.S.A, pp. 1042-1051.
- [6] Horsley, D. J., 2003, "Background to the use of CTOA for Prediction of Dynamic Ductile Fracture Arrest in Pipelines", Engineering Fracture Mechanics, 70, pp. 547-552.
- [7] Mannucci, G., Buzzichelli, G., Salvini, P., Eiber, R., and Carlson, L., 2000, "Ductile Fracture Arrest Assessment in a Gas Transmission Pipeline using CTOA", Proc. 2nd International Pipeline Conference, Calgary, Alberta, Canada, ASME, 1, pp. 315-320.
- [8] Wilkowski, G. M., Rudland, D. L., Wang, Y. Y., Horsley, D., Glover, A., and Rothwell, B., 2002, "Determination of the Region of Steady State Crack Growth from Impact Tests", Proc. 4th International Pipeline Conference, paper No. IPC04-27132, Calgary, Alberta, Canada, pp. 1-7.
- [9] ASTM Standard E1876-01, "Standard Test Method for Dynamic Young's Modulus, Shear Modulus, and Poisson's Ratio by Impulse Excitation of Vibration", 100 Barr Harbor Drive, ASTM Book of Standard Volumes 03.01, West Conshohocken, PA, 19428.
- [10] Shterenlikht, A., Hashemi, S. H., Howard, I. C., Yates, J. R., and Andrews, R. M., 2004, "A specimen for studying the resistance to ductile crack propagation in pipes", Engineering Fracture Mechanics, 71, pp. 1997-2013.
- [11] Hashemi, S. H., Gay, R., Howard, I. C., Andrews, R. M., and Yates, J. R., 2004, "Development of a Laboratory Test Technique for Direct Estimation of Crack Tip Opening Angle", Proc. 15th European Conference of Fracture, Stockholm, Sweden.
- [12] ASTM Standard E1290-99, 2002, "Standard Test Method for Crack Tip Opening Displacement (CTOD) Fracture Toughness Measurement," 100 Barr Harbor Drive, ASTM Book of Standard Volumes 03.01, West Conshohocken, PA, 19428.
- [13] Burton, W., Mahmoud, S., and Lease, K., 2004 "Effects of Measurements Techniques on the Experimental Characterization of Crack tip Opening Angle - Δa Resistance Curves", Society for Experimental Mechanics, 44 (4), pp. 425-432.
- [14] Ma, L., Kobayashi, A. S., Atluri, S. N., and Tan, P. W., 2002, "Crack Linkup: An Experimental Analysis", Experimental Mechanics, 42 (2), pp. 147-152.
- [15] Mahmoud, S., and Lease, K., 2003, "The effect of the specimen thickness on the experimental characterization of critical crack-tip-opening angle in 2024-T351 aluminium alloy", Engineering Fracture Mechanics, 70, pp. 443-456.
- [16] Schwalbe, K.-H., Newman, J. C. Jr., Shannon, J. L. Jr., 2005, "Fracture mechanics testing on specimens with low constraint–standardisation activities within ISO and ASTM", Engineering Fracture Mechanics, 72, pp. 557-576.
- [17] Mannucci, G., and Harris, D., 2002, "Fracture Properties of API X100 Pipeline Steels", Report No. EUR 20330 EN, European Communities.
- [18] Berardo, G., Salvini, P., Mannucci, G., and Demofonti, G., 2000, "On Longitudinal Propagation of a Ductile Fracture in a Buried Gas Pipeline: Numerical and Experimental Analysis", Proc. 2nd International Pipeline Conference, Calgary, Alberta, Canada, ASME, 1, pp. 287-294.
- [19] Swenson, D. V., and James, M. A., 1996, "FRANC2D/L: A Crack Propagation Simulator for Plane Layered Structures", Version 1.4 User's Guide, Kansas State University, Manhattan, Kansas, U.S.A.
- [20] James, M. A., 1998, "A Plane Stress Finite Element Model for Elastic-Plastic Mode I/II Crack Growth", Ph.D. Thesis, Kansas State University, Kansas, U.S.A.
- [21] Newman, J. C. Jr., Shivakumar, K. N., and McCabe, D. E., 1991, "Finite Element Fracture Simulation of A533B Steel Sheet Specimens", Proc. ESIS/EGF9, Defect Assessment in Components – Fundamentals and Application, J. G. Blauel and K.-H. Schwalbe, eds., Mechanical Engineering Publication, London, pp. 117-126.
- [22] Newman, J. C. Jr., Dawicke, D. S., Sutton, M. A., and Bigelow, C. A., 1993, "A Fracture Criterion for Widespread Cracking in Thin-Sheet Aluminum Alloys", Proc. 17th International Committee on Aeronautical Fatigue, pp. 443-468.
- [23] Dawicke, D. S., 1996, "Residual Strength Predictions Using a CTOA Criterion", Proc. FAA-NASA Symposium on Continued Airworthiness of Aircraft Structures, Atlanta, GA.
- [24] Newman, J. C. Jr., Booth, B. C., and Shivakumar, K. N., 1988, "An Elastic-Plastic Finite-Element Analysis of the J -resistance Curve using a CTOD Criterion", Proc. Fracture Mechanics: Eighteenth Symposium, ASTM STP 945, D.T. Read and R.P. Reed, eds., American Society for Testing and Materials, Philadelphia, pp. 665-685.